Transport of Loaded and Unloaded Microcarriers in a Colloidal Magnetic Shift Register

Pietro Tierno,*,† Sathavaram V. Reddy,† Jing Yuan,† Tom H. Johansen,‡ and Thomas M. Fischer*,†,§

Department of Chemistry and Biochemistry, Florida State University, Tallahassee, Florida 32306-4390, Department of Physics, University of Oslo, P. O. Box 1048, Blindern, Norway, and Institut für Experimentalphysik V, Universität Bayreuth, 95440 Bayreuth, Germany

Received: July 16, 2007; In Final Form: September 4, 2007

We demonstrate the dispersion free digital transport of emulsion droplets and biological cells in an aqueous solution using paramagnetic colloidal particles above a uniaxial magnetic garnet film. Magnetic modulations above the stripe domain pattern induce a step-wise transport of paramagnetic particles dispersed in water and deposited on the surface of the film. Capillary or hydrodynamic interactions are then used to couple the cargo to the paramagnetic beads. We achieve full control of the cargo motion up to velocities in the 100 μm/s range.

Introduction

Detection and manipulation of emulsion droplets or biological cells by colloidal carriers is a promising approach toward controlled release and site-specific delivery of drugs. Use of surface reactive groups on the colloidal particles allows the linkage with nucleic acids,[1] cells,[2] or polymer molecules.[3] Moreover, successful delivery of the particle's cargo on the smaller scale requires that the individual particles are distinguishable from their neighbors and thus the colloidal carrier assembly to move dispersion free toward the target site. The particles can then be manipulated with the aid of noninvasive external (electric,[4] magnetic,[5] or optical[6]) fields that transport the particles toward a defined location on the microfluidics device. Magnetic field manipulation is often preferred over optical or electric manipulation because magnetic fields have minor effects on the often precious biological cargo.[6] Magnetic colloidal particles have recently been used in magnetic resonance imaging and magnetically guided drug delivery.[7] A rich variety of magnetic manipulation techniques like magnetic tweezers,[8] microcoil,[9] micromagnetic systems,[10] array of permalloy elements,[11] or electromagnetic traps[12] has therefore been developed. Helseth et al.[15] found that domain walls in ferrimagnetic garnet films generate magnetic fields heterogeneous on the colloidal scale that provide all the requirements needed for a simple magnetic manipulation of paramagnetic particles and their cargo. When an aqueous solution of the particles is placed on top of a garnet film, the particles are pinned to the domain walls by the stray magnetic field of the film. Application of an external magnetic field changes the domain distribution in the garnet film and thus moves the particle in a determined direction.

On the basis of these ideas we developed a dispersion-free magnetic colloidal shift register that digitally drives a large ensemble of colloidal particles[13] across the stripe pattern of the garnet film. We deposited paramagnetic particles (2.8 μm in diameter) on the parallel stripes domains of a ferrimagnetic garnet film. In the absence of an external field the particles deposit on the domain walls to form consecutive lines. Simple time-dependent magnetic field pulses sequentially shift the whole 2D colloidal assembly by one period of the magnetic domain pattern. The induced digital motion (one magnetic period per pulse) conserves the order of the particles along each line.

Here we focus on the transport properties of the shift register and use the colloidal particles as microscopic carriers for micrometer-sized chemical or biological units. First we attach small oil droplets to the particles and transport them in a defined location on the platform with speeds up to 200 μm/s. Then we use the secondary flow generated by the moving array of particles to drag yeast cells in the particle direction. In the second case the cells are not attached to the particles and can be transported up to 100 μm/s. The force required by the shift register to move the particle is on the order of pN. This force must balance the viscous force and dictates the volume of liquid, oil droplets, or cells to be transported, while the number and size of the particles dictate the amount of fluid displaced. Both characteristics finally determine the efficiency of the device in possible lab-on-a chip applications, as discussed in the present work.

Experimental Section

The stripe pattern for the particle motion was created using a uniaxial magnetic garnet film of composition $Y_{2.5}Bi_{0.5}Fe_{5-q}Ga_qO_{12}$ ($q = 0.5-1$), thickness 5 μm, and saturation magnetization $M_s = 1.7 \times 10^4$ A/m. The garnet film was grown by liquid-phase epitaxy on a GGG (gadolinium gallium garnet) substrate of 0.5 mm thickness. The film has an area of 0.25 cm^2 and was deposited with its substrate on top of a plastic container. The garnet, which is compatible with any glass, plastic, or metallic substrate, can be easily integrated in a microfluidic device. A series of alternating ferromagnetic domains with up and down magnetization direction can be visualized using polarization microscopy (Faraday effect). Each stripe domain has size $\lambda/2$, where $\lambda = 10.9$ μm is the wavelength of the stripe pattern. Application of an external magnetic field normal to the film increases (decreases) the size of the domain with parallel (antiparallel) magnetization direction.[14]

* To whom correspondence should be addressed. E-mail: tfischer@chem.fsu.edu.
† Florida State University.
‡ University of Oslo.
§ Universität Bayreuth.

10.1021/jp0755589 CCC: $37.00
Published on Web 11/13/2007 PAGE EST: 3.5

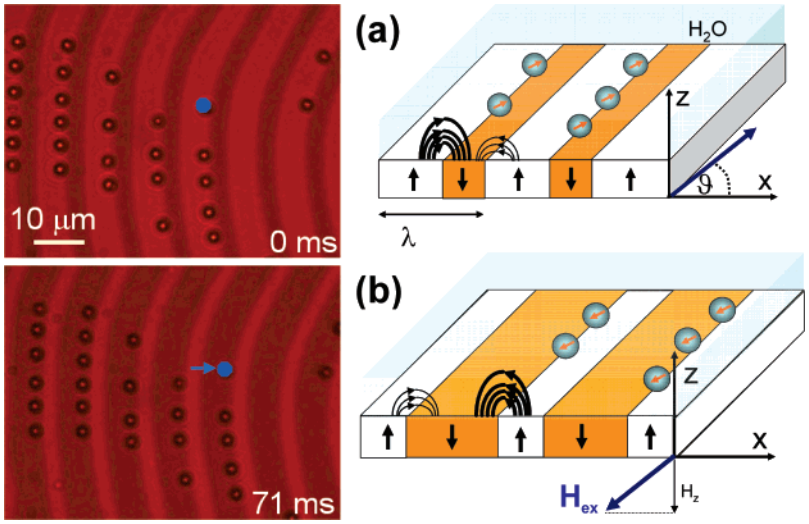

Figure 1. Mechanism of the colloidal shift register: Reversing the magnetic field converts strong domain walls into weak domain walls and the particles hop by one stripe during a half cycle (schematics to the right). To the left we show two corresponding polarization microscopy images of the stripe pattern with the particles. One particle is marked in blue. The corresponding movie of the hopping can be found in the Supporting Information.

The colloids used are paramagnetic polystyrene particles with a mean diameter of 2.8 ± 0.1 μm, density $\rho = 1.4$ g/cm^3, and effective magnetic susceptibility $\chi = 0.17$ (Dynabeads M-270). In water the particles acquire a negative charge due to dissociation of the surface carboxylic groups (COO^-). To prevent adhesion of the particles to the garnet film, we coat the film with a thin layer of polysodium-4-stryrene sulfonate.[15] We dilute the original particle solution with deionized water (18.2 MΩ·cm, Milli Q system) to a concentration of 10^7 particle/mL (particle stock solution).

Oil Droplets. To attach oil droplets to the particles we prepared a dispersion of 1.02% by wt silicon-oil (Fisher scientific) in water. This solution was then mixed one to one with the particle stock solution and sonicated for 15 min. Sonication formed an emulsion of oil droplets from 0.5 to 10 μm in size in which some of the droplets attach to the particles. The corresponding solution was then placed on top of the garnet film.

Yeast Cell. The budding yeast cells (*Saccharomyces cerevisiae*) were first centrifuged from the YPD culture media (10 g of BactoYeast extract, 20 g of BactoPeptone, and 20 g of Dextrose in 1 L of water) and then re-suspended with deionized water to a concentration of 10^6 cells/mL. The resulting solution was mixed 3 to 1 with the particle stock solution before deposition on the garnet film.

Methods. The external magnetic field was applied using two coils with the main axis along the x and z direction, and field modulations were achieved using a wave generator feeding an amplifier. The particles and droplets or cells were visualized using a Leica, DMPL polarization microscope working in transmission mode. Videos of the colloidal kinetics were taken either at 30 fps using a color camera (Basler VT) or at 125 fps with a black and white camera (Fastcam Super 10 K Photronat). Tracking was realized with freeware image processing software (Imagej).

Results

In Figure 1 we show two polarization microscopy images and a schematic that describes the principle of the magnetic shift register. When placed above the garnet film, the paramagnetic particles are pinned on top of the domain wall by the stray magnetic field. When superimposing an in-plane field perpendicular to the stripes the magnetic field above the domain walls alternates between strong and weak pinning such that the particles are forming consecutive lines above the strong pinning domain walls. To move the particle in a defined direction, we applied oscillating magnetic field pulses in the (x,z) plane, $H_{ext} = \hat{H}(\sin \omega t, 0, \sin \omega t)$ with frequency 6 s^{-1} < ω < 125 s^{-1}, amplitude $\hat{H} = 1.3 \times 10^4$ A/m, and inclination $\vartheta = 45°$ with respect to the z axis. The component of the field normal to the film displaces the domain wall by increasing the width of the domains having parallel magnetization direction. Hopping across the domains occurs because the pinning sites alternate between weak and strong during the magnetic modulation of the planar component of the field. This is illustrated in the schematic of Figure 1 by the direction and intensity (line thickness) of the magnetic field line at the domain wall. The particle motion is always directed normal to the stripe pattern. The particles move by one wavelength λ during one field cycle (Figure 1 shows one-half a cycle). The hopping from one to the next wall renders the longitudinal motion free of dispersion. Individual differences in speed due to different drag coefficients are erased after each hop. This ensures that the particles do not separate along the direction of motion and they all move with a defined speed, $v_p = \lambda\omega/2\pi$. We deposited a movie showing the digital particle motion in the Supporting Information.

The magnetic shift register can be used to transport liquid droplets as cargo attached to the particles. In Figure 2a we show a schematic of a spherical droplet attached to the particle on top of the garnet film. The small inset illustrates the force balance at the water/particle/oil interface, where ϑ is the three-phase contact angle. The magnetic force, F_m, on the particle is given by the local magnetic field gradient

$$\vec{F}_m = \mu(\vec{m}\cdot\nabla)\vec{H}$$

where μ is the magnetic permeability of water, $\vec{m} = V\chi\vec{H}$ is the particle magnetic moment, V the volume of the magnetic particle core, and $\vec{H} = \vec{H}_{ext} + \vec{H}_{garnet}$, the total magnetic field. In the x direction and distance z above the garnet surface, the field is given by[13]

$$H_x(x,z) = \frac{1}{\pi}\cdot\mathrm{Re}\left(\frac{\sin(\pi(x+iz) - \pi\hat{H}_{ext}\cos\phi/4)i}{\cos(\pi(x+iz) + \pi\hat{H}_{ext}\cos\phi/4)} + \pi\hat{H}_{ext}\sin\phi\right)$$

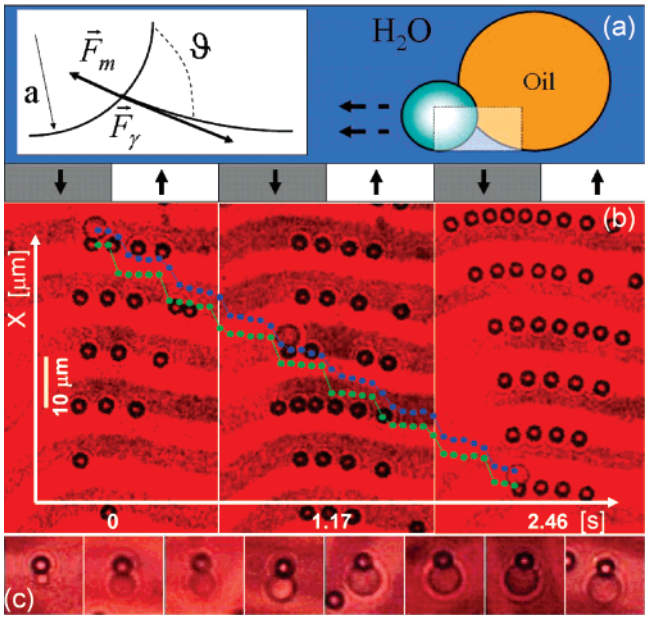

Figure 2. (a) Schematic showing the colloidal particle and oil droplet on the stripe pattern of the garnet film. Inset shows the force diagram at the three-phase (water/oil/particle) contact line. (b) Polarization microscopy images of the particles and oil droplet on the garnet film. The *x* position of one colloidal particle in green and oil droplet in blue is depicted as a function of time. (c) Different images showing differently sized droplets that can be transported by the particles. A corresponding movie of the oil-droplet transport can be found in the Supporting Information.

where we are using dimensionless units.[16] It follows that the magnetic forces are in the nN range. Capillary numbers are small, on the order of Ca $\approx 10^{-6}$. Thus, once an oil droplet is attached to a particle, its shape remains circular and it cannot be detached from the carrier particle by the viscous forces. This allows transporting the oil droplet with high particle speed $v = \lambda\omega/2\pi \approx 200$ μm/s. The discrete time-based motion of the particle (green) and cargo (blue) is shown in Figure 2b. Figure 2c shows different attoliter-sized oil droplets of volume ranging from 10^{-17} to 10^{-19} L that can be transported in this way. The limitation on the volume is given by the size of the particle used. The size of the particles, in turn, decides the choice of wavelength of the particular stripe pattern garnet film to be used. Larger (smaller) particles combined with a garnet film having larger (smaller) stripe periods allow an increase (decrease) of the amount of fluid transported. However, too large oil droplets will deposit and stick to the garnet surface, thus restraining this transport mechanism to emulsion droplets smaller than 8.5 μm in diameter.

The magnetic shift register can be used also for the transport of biological cells. To avoid an invasive approach like incorporation of the paramagnetic particle into the cell,[17] we used the secondary flow generated by the particle motion for the transport of yeast cells (*Saccharomyces cerevisiae*). Seen in Figure 3a are three polarization microscopy images showing the position of the paramagnetic particles and the yeast cells at different times. We superimpose the trajectory of one colloidal particle in green and one yeast cell in blue. During motion the particles generate a flow which drags the cells in the same direction. In contrast to the oil droplet motion more particles are needed to generate sufficient secondary flow. Once deposited on the garnet, the yeast cells levitate 1−2 μm above the particles, probably because of their lower density ($\rho = 1.1$ g/cm^3) and no attraction toward the domain wall, Figure 3c. The particles move below the cells but do not stick to them due to double layer repulsion (yeast cell in water acquires a negative charge[18]). Plotted in Figure 3b is the speed of the particle, v_p, versus the speed of the cell, v_d, and we observe a linear behavior up to 110 μm/s. The yeast cells roughly move with one-half the speed of the particles. The viscous drag force $F_{drag} \approx 6\pi\eta R v_p$ experienced by the yeast cell can be calculated from the Stokes equation where $\eta \approx 10^{-3}$ Pas is the water viscosity and $R \approx 2.3$ μm is the radius of the cell. We estimate this force to be on the order of 0.4−7.5 pN for a field frequency of $\omega = 6.2-$

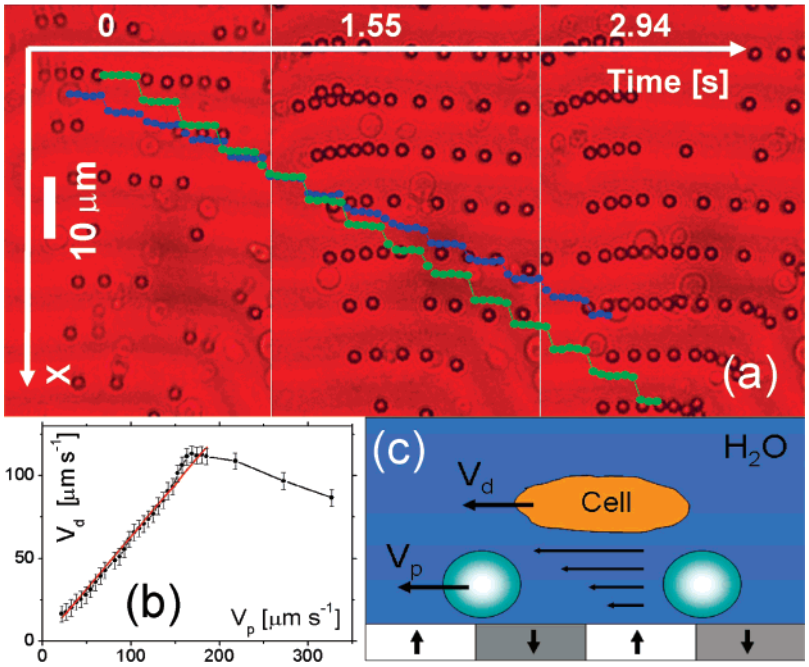

Figure 3. (a) Polarization microscopy sequence of colloidal particles transporting yeast cells by secondary flow. In green is the *x* position of one particle and in blue of one yeast cell as a function of time. (b) Velocity of the yeast cell v_d versus the particle velocity v_p; the red line is a linear fit. (c) Schematic showing the particle and cell position on top of the garnet film. The corresponding movie showing the advection of the yeast cells can be found in the Supporting Information.

125.7 s^{-1}. The direction of the flow field generated by the moving array of particle can be easily reversed by changing the magnetic field polarity. This method for the transport of biological cells can be extended, in principle, to any other cell in this size range.

Conclusions

We realized a magnetic shift register for the digital dispersion-free transport and delivery of microscopic objects such as oil droplets or yeast cells. The noninvasive external magnetic field modulation enables transporting objects that are either directly attached to their carrier particle or advected by the secondary flow generated by the particle assembly. Typical magnetic forces needed to transport the particles are in the range of pN. Our system can be used for microfluidic devices. Variation of the stripe domain wavelength allows the technique to be miniaturized to the nanometer scale which will be useful when dealing with ever smaller amounts of material.

Acknowledgment. We thank Yanchang Wang and Xianying Tang for providing the yeast cells. This material is based upon work supported by the National Science Foundation under CHE-0649427. T.H.J. thanks The Research Council of Norway for financial support.

Supporting Information Available: Videos corresponding to the image sequences in Figures 1−3: (1) Hopping.mpeg, video showing the hopping adobe the garnet stripe pattern (Figure 1); (2) Oil drop.mpeg, video showing the transport of the oil drop (Figure 2); (3) Yeast cell.mpeg, video showing the transport of the yeast cells (Figure 3). This material is available free of charge via the Internet at http://pubs.acs.org.

References and Notes

(1) Valignat, M. P.; Olivier, T.; Crocker, J. C.; Russel, W. B.; Chaikin, P. M. *Proc. Nat. Acad. Sci.* **2005**, *102*, 4225.

(2) Dreyfus, R.; Baudry, J.; Roper, M. L.; Fermigier, M.; Stone, H. A.; Bibette, J. *Nature* **2005**, *437*, 862.

(3) Xu, H.; Yan, F.; Tierno, P.; Marczewski, D.; Goedel, W. A. *J. Phys. Condens. Matter* **2005**, *17*, S465.

(4) Hayward, R. C.; Saville, D. A.; Aksay, I. A. *Nature* **2000**, *404*, 56.

(5) Yellen, B. B.; Hovorka, O; Friedman, G. *Proc. Nat. Acad. Sci.* **2005**, *102*, 25.

(6) Terray, A.; Oakey, J.; Marr, D. W. M.; *Science*, **2002**, *296*, 1841.

(7) Zimmer, C.; Wright, S. C., Jr.; Engelhardt, R. T.; Johnson, G. A.; Kramm, C.; Breakefield, X. O.; Weissleder, R. *Exp. Neurol.* **1997**, *143*, 61.

(8) Haber, C.; Wirtz, D. *Rev. Sci. Instrum.* **2000**, *71*, 4561.

(9) Rogers, J. A.; Jackman, R. J.; Whitesides, G. M.; Olson, D. L.; Sweedler, J. V. *Appl. Phys. Lett.* **1997**, *70*, 2464.

(10) Deng, T.; Whitesides, G. M.; Radhakrishnan, M.; Zabow, G.; Prentiss, M. *Appl. Phys. Lett.* **2001**, *78*, 1775.

(11) Mirowski, E.; Moreland, J.; Russek, S. E.; Donahue, M. J. *Appl. Phys. Lett.* **2004**, *84*, 178.

(12) Lee, C. S.; Lee, H.; Westervelt, R. M. *Appl. Phys. Lett.* **2001**, *79*, 3308.

(13) Tierno, P.; Reddy, S. V.; Johansen, T. H.; Fischer, T. M. *Phys Rev. E* **2007**, *75*, 041404.

(14) Helseth, L. E.; Backus, T.; Johansen, T. H.; Fischer, T. M. *Langmuir* **2005**, *21*, 7518.

(15) Helseth, L. E.; Wen, H. Z.; Fischer, T. M.; Johansen, T. H. *Phys. Rev. E* **2003**, *68*, 011402.

(16) H is measured in units of the saturation magnetization M_s and x and y in units of the wavelength λ.

(17) Hosu, B. G.; Jakab, K.; Bánki, P.; Tóth, F. I.; Forgacs, G. *Rev. Sci. Instrum.* **2003**, *74*, 4158.

(18) Powell, C. D.; Quain, D. E.; Smart, K. A. *FEMS Yeast Res.* **2003**, *3*, 149.